ORIGINAL RESEARCH

MRI Features for Predicting Microvascular Invasion and Postoperative Recurrence in Hepatocellular Carcinoma Without Peritumoral Hypointensity

Zhiyuan Chen[1,*], Xiaohuan Li[2,*], Yu Zhang[2], Yiming Yang[1], Yan Zhang[3], Dongjing Zhou[1], Yu Yang[4], Shuping Zhang[1], Yupin Liu [ID][1]

[1]Department of Radiology, The Second Affiliated Hospital of Guangzhou University of Chinese Medicine, Guangzhou, Guangdong, 510120, People's Republic of China; [2]The Second Affiliated Hospital of Guangzhou University of Chinese Medicine, Guangzhou, Guangdong, 510120, People's Republic of China; [3]Integrated Department, the Second Affiliated Hospital of Guangzhou University of Chinese Medicine, Guangzhou, Guangdong, 510120, People's Republic of China; [4]Department of Pathology, the Second Affiliated Hospital of Guangzhou University of Chinese Medicine, Guangzhou, Guangdong, 510120, People's Republic of China

*These authors contributed equally to this work

Correspondence: Yupin Liu, Department of Radiology, the Second Affiliated Hospital University of Guangzhou Traditional Chinese Medicine, No. 111 Dade Road, Yuexiu District, Guangzhou, Guangdong, 510120, People's Republic of China, Tel +8613688878398, Fax +862034728881, Email mdliuyupin@163.com

Video Abstract

Point your SmartPhone at the code above. If you have a QR code reader the video abstract will appear. Or use: https://youtu.be/n3MU15ZJfBM

Purpose: To identify MRI features of hepatocellular carcinoma (HCC) that predict microvascular invasion (MVI) and postoperative intrahepatic recurrence in patients without peritumoral hepatobiliary phase (HBP) hypointensity.

Patients and Methods: One hundred and thirty patients with HCC who underwent preoperative gadoxetate-enhanced MRI and curative hepatic resection were retrospectively reviewed. Two radiologists reviewed all preoperative MR images and assessed the radiological features of HCCs. The ability of peritumoral HBP hypointensity to identify MVI and intrahepatic recurrence was analyzed. We then assessed the MRI features of HCC that predicted the MVI and intrahepatic recurrence-free survival (RFS) in the subgroup without peritumoral HBP hypointensity. Finally, a two-step flowchart was constructed to assist in clinical decision-making.

Results: Peritumoral HBP hypointensity (odds ratio, 3.019; 95% confidence interval: 1.071–8.512; *P*=0.037) was an independent predictor of MVI. The sensitivity, specificity, positive predictive value, negative predictive value, and AUROC of peritumoral HBP hypointensity in predicting MVI were 23.80%, 91.04%, 71.23%, 55.96%, and 0.574, respectively. Intrahepatic RFS was significantly shorter in patients with peritumoral HBP hypointensity (*P*<0.001). In patients without peritumoral HBP hypointensity, the only significant difference between MVI-positive and MVI-negative HCCs was the presence of a radiological capsule (*P*=0.038). Satellite nodule was an independent risk factor for intrahepatic RFS (hazard ratio,3.324; 95% CI: 1.733–6.378; *P*<0.001). The high-risk HCC detection rate was significantly higher when using the two-step flowchart that incorporated peritumoral HBP hypointensity and satellite nodule than when using peritumoral HBP hypointensity alone (*P*<0.001).

Conclusion: In patients without peritumoral HBP hypointensity, a radiological capsule is useful for identifying MVI and satellite nodule is an independent risk factor for intrahepatic RFS.

Keywords: hepatocellular carcinoma, microvascular invasion, postoperative recurrence, peritumoral hypointensity, magnetic resonance imaging

Introduction

Hepatocellular carcinoma (HCC) is the fifth most common malignancy and the third leading cause of cancer-related deaths worldwide, with a relative 5-year survival rate of approximately 18%.[1,2] China has a high burden of liver cancer,

1595

with 45.3% of liver cancer cases and 47.1% of liver cancer deaths globally.[3] Radical resection is the main curative treatment for HCC. However, more than half of the patients treated with R0 resection will develop recurrence,[4] which has a strong impact on prognosis. Microvascular invasion (MVI), defined as the presence of clusters of tumor cells in vessels located in the peritumoral area of the liver,[5] is a major risk factor for HCC recurrence after surgery. However, MVI can only be detected by microscopic examination of the surgical specimen, which limits its application, particularly in terms of preoperative therapeutic decision-making and determination of resection margins during hepatectomy. Therefore, it is of great value to explore noninvasive methods that can determine MVI status preoperatively.

Several noninvasive preoperative methods, including radiomics, deep learning, and gene expression signatures, have been used to predict MVI status and early tumor recurrence. Gadolinium ethoxybenzyl diethylenetriamine pentaacetic acid (Gd-EOB-DTPA)-enhanced MRI is widely used for the diagnosis and assessment of HCC. Assessment of tumor features on Gd-EOB-DTPA-enhanced MRI is easy to perform and does not require additional devices or expenses. Owing to the lack of organic anion-transporting polypeptide (OATP) transporter expression, most HCCs present hypointense signal compared to the surrounding liver parenchyma on hepatobiliary phase (HBP) imaging. In MVI-positive patients, tumor cells in the vessels can result in dysfunction of the OATP transporter in hepatocytes located in the peritumoral liver parenchyma, leading to peritumoral HBP hypointensity. Although peritumoral HBP hypointensity has been identified as an important imaging feature with high specificity for predicting MVI, its sensitivity is relatively poor and was found to be only 44.2% in a recent meta-analysis.[6,7] This finding indicates that more than half of patients with MVI do not show peritumoral HBP hypointensity. Given the importance of MVI in HCC management, it is imperative to identify complementary features that can predict MVI and tumor recurrence in patients without peritumoral HBP hypointensity. To the best of our knowledge, few studies have focused on this topic or its population.

Therefore, this study aimed to identify the MRI features of HCC that predict MVI and postoperative recurrence in patients without peritumoral HBP hypointensity.

Materials and Methods
Patients
This retrospective study was compliant with the ethical guidelines of the 1975 Declaration of Helsinki and approved by the ethics committee of the Second Affiliated Hospital of Guangzhou University of Chinese Medicine. The requirement for written informed consent was waived by the Institutional Review Board owing to the retrospective observational nature of the study, and all patient data are treated confidentially. The data of treatment-naive patients who underwent preoperative liver Gd-EOB-DTPA-enhanced MRI and curative hepatic resection for HCC at our institution between December 2017 and December 2021 were reviewed. The inclusion criteria were age >18 years and presence of a single histopathologically confirmed HCC lesion. The following exclusion criteria were applied: (1) more than a 2-month interval between Gd-EOB-DTPA-enhanced MRI and surgery, (2) suboptimal MRI quality, (3) pathologically confirmed macroscopic vascular invasion, (4) extrahepatic spread on preoperative work-up, (5) incomplete clinical and laboratory data, (6) lack of follow-up data, and (7) history of preoperative HCC-related treatment (chemotherapy, radiotherapy, transarterial chemoembolization, radiofrequency ablation, or immunosuppressive therapy).

MRI Protocol
Patients underwent upper abdominal MRI using two 3.0-T MRI vectors with an 8-channel Atlas Speeder phased-array coil (Titan; Toshiba Medical Systems, Tochigi, Japan) or 18-channel phased-array coil (Prisma; Siemens Healthcare, Erlangen, Germany). All patients fasted for at least 8 h before MRI examination. Axial T1-weighted, T2-weighted, and dynamic contrast-enhanced images were obtained in all the cases. Each patient received 0.1 mL/kg of gadoxetic acid disodium (Primovist; Bayer Vital GmbH, Berlin, Germany) at a flow rate of 2 mL/s to acquire Gd-EOB-DTPA-enhanced images. Arterial phase, portal phase, and HBP images were obtained 15 s, 60–70 s, and 20 min after contrast injection, respectively. The acquisition parameters are listed in Table S1.

Interpretation of Images

Two board-certified radiologists (X.H.L. and Y.M.Y., with 5 and 10 years of experience in liver MRI, respectively), who were blinded to the histopathological results, laboratory data, and follow-up information, independently reviewed all preoperative MRI scans. They were required to count the number, measure the longest diameter of each target observation, and classify the imaging features of each HCC lesion. Two weeks before the formal assessment, they were required to discuss the presentation of each MRI feature, and were trained in 20 cases. The definition of imaging features on Gd-EOB-DTPA-enhanced MRI has been described in other studies and is documented in Table S2.[8–10] The interobserver agreement was assessed after independent image review. In the event of disagreement between the two radiologists, a senior radiologist (Z.Y.C., with 15 years of experience in liver MRI) reviewed the images and discussed them with the other two radiologists, and a consensus was reached by a majority vote.

Clinical and Laboratory Data

Clinical (age, sex, etiology of chronic liver disease) and laboratory data (white blood cells [WBC], red blood cells [RBC], hemoglobin [HB], platelets [PLT], prothrombin time [PT], international normalized ratio of prothrombin [INR], activated partial thromboplastin time [APTT], fibrinogen [FIB], alanine aminotransferase [ALT], aspartate transaminase [AST], albumin [ALB], globulin [GLB], alkaline phosphatase [ALP], gamma-glutamyltransferase [GGT], total bilirubin [TBIL], creatinine [Cr]), and serum alpha-fetoprotein [AFP]) within 1 week before hepatectomy were reviewed. The Child-Turcotte-Pugh (CTP) stage and Model for End-Stage Liver Disease (MELD) score were calculated for each patient according to the American Association for the Study of Liver Disease (AASLD) guidelines.[11]

Histological Evaluation

After surgical resection, formalin-fixed paraffin-embedded specimens were stained with hematoxylin and eosin and evaluated by a senior pathologist with 15 years of experience in liver pathology, according to the seven-point baseline sampling protocol. Histopathological reports included tumor number, tumor size, Edmondson grade, MVI status, and final diagnosis. MVI was defined as the presence of tumor cells in the endothelium-lined vascular lumen observed only by microscopy.

Follow-Up After Surgical Resection

All patients underwent clinical and radiological follow-up at 1 month after hepatectomy, at 3-month intervals for the first 2 years, and at 6-month intervals for up to 5 years thereafter. Radiological follow-up consisted of ultrasonography, dynamic-enhanced computed tomography, or Gd-EOB-DTPA-enhanced MRI. When recurrence was suspected clinically or radiologically, appropriate management was implemented according to our institutional protocol and the AASLD guidelines. Patients were censored in the event of local recurrence, loss to follow-up, or on March 1, 2023, whichever event occurred first. Intrahepatic recurrence-free survival (RFS) was defined as the time interval between hepatectomy and intrahepatic recurrence.

Statistical Analysis

Continuous variables were reported as the mean ± standard deviation or median (interquartile range [IQR]) and were compared between groups using Student's *t*-test or Mann–Whitney *U*-test, as appropriate. Categorical variables were reported as frequency (percentage) and compared between groups using the chi-square test or Fisher's exact test, as appropriate. Interobserver agreement regarding MRI features was assessed using the Cohen's kappa (κ) value and graded based on the Landis and Koch scale (0.00, poor agreement; 0.01–0.20, slight agreement; 0.21–0.40, fair agreement; 0.41–0.60, moderate agreement; 0.61–0.80, substantial agreement; and >0.80, nearly perfect agreement).[12]

The relationship between radiological variables and MVI status was assessed using univariate logistic regression analysis. Variables with a *P*-value <0.05 in univariate analysis were entered into multivariate logistic regression analysis with stepwise forward selection to identify independent risk factors. Prediction performance was assessed by measuring the area under the receiver operating characteristic curve (AUROC), odds ratio (OR) with 95% confidence interval (CI),

sensitivity, specificity, positive predictive value (PPV), and negative predictive value (NPV). Subgroup analysis was performed for patients without peritumoral HBP hypointensity, using the same methods.

Postoperative intrahepatic RFS was estimated using the Kaplan–Meier method, and survival curves were compared using the Log rank test. The prognostic value of MRI features for postoperative intrahepatic RFS in the subgroup of patients without peritumoral HBP hypointensity was evaluated using univariate and multivariate Cox proportional hazards regression analyses and quantified using the hazard ratio (HR).

All statistical analyses were performed using SPSS (version 22.6; IBM Corp., Armonk, NY, USA) and MedCalc (version 16.8.4; Ostend, Belgium). Statistical significance was defined as a two-sided P-value <0.05.

Results

Patients

One hundred and thirty of 315 patients who underwent curative resection for HCC during the study period were enrolled (Figure 1). The median age was 55.0 years (IQR 47.0–63.0), 114 patients (87.7%) were male, the most common etiology of liver disease was chronic hepatitis B (84.6%), and 63 patients (48.5%) were MVI-positive. Edmondson grade III or IV was more common in the MVI-positive group than in the MVI-negative group. There were no other significant differences in the clinical or pathological characteristics between the two groups (Table 1).
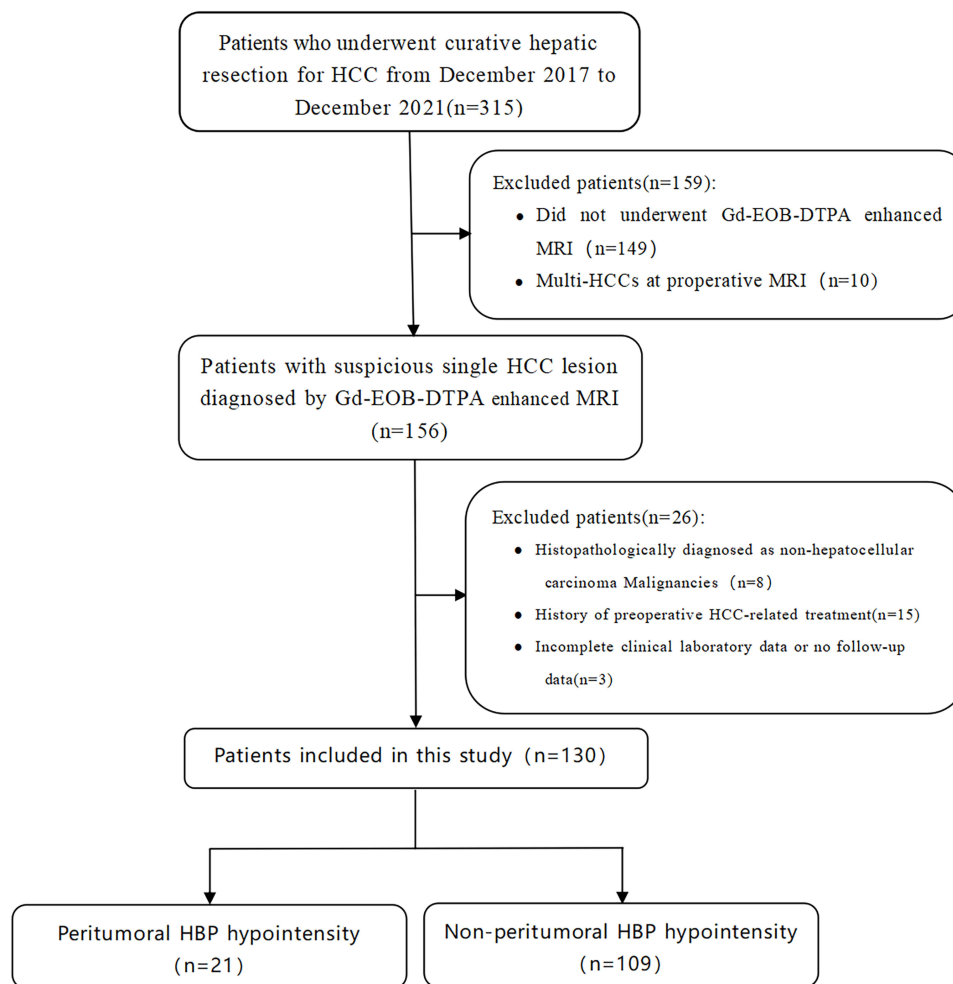

Figure 1 Flowchart showing the patient inclusion and exclusion criteria.

Table 1 Clinical and Pathological Characteristics of MVI-Positive and MVI-Negative Cohorts

Characteristic	MVI Positive (n=63)	MVI Negative (n=67)	*P* value
Age (year)	55.0±11.3	55.6±11.4	0.805
Gender			0.184
Female	5(7.9%)	11 (16.4%)	
Male	58(92.1%)	56 (83.6%)	
Etiology of liver disease			0.703
Hepatitis B	52(82.5%)	58(86.6%)	
Hepatitis C	7(11.1%)	7(10.4%)	
No or other	4(6.3%)	2(3.0%)	
WBC (×10^9/L)	6.06(5.17–7.43)	5.71(4.50–6.73)	0.156
RBC (×10^{12}/L)	4.67±0.60	4.77±0.68	0.384
HB (g/L)	147(130–155)	142(130–152)	0.545
PLT (×10^9/L)	170(138–215)	178(132–220)	0.929
PT (s)	13.2±1.3	12.9±1.3	0.169
INR (R)	1.02(0.96–1.08)	1.03(0.97–1.11)	0.400
APTT(s)	35.8(28.5–40.1)	36.8(32.6–39.7)	0.584
FIB (g/L)	2.92(2.50–3.66)	2.89(2.48–3.39)	0.631
ALT (U/L)	28.0(20.0–42.5)	26.0(18.0–42.0)	0.531
AST (U/L)	29.0(21.0–50.0)	27.0(22.0–41.0)	0.702
ALB (g/L)	43.2±4.4	43.3±4.3	0.945
GLB (g/L)	28.6±4.6	28.9±4.5	0.655
ALP (U/L)	80(65.5–113.0)	84.0(68.5–107.0)	0.718
GGT (U/L)	52.0(31.5–97.0)	50.0(26.5–100.0)	0.730
TBIL (μmol/L)	11.8(8.9–15.4)	11.9(8.4–15.9)	0.716
Cr (μmol/L)	81.0(70.0–89.0)	80.0(67.0–88.0)	0.658
AFP (ng/mL)	14.0(4.3–222.2)	17.0(4.9–375.6)	0.628
CTP	5.0(5.0–6.0)	5.0(5.0–6.0)	0.438
MELD	4.52(3.03–5.70)	4.26(1.79–6.53)	0.757
Edmondson grade			<0.001
I	1 (1.6%)	4 (6.0%)	
II	17 (27.0%)	40 (59.7%)	
III	37 (58.7%)	22 (32.8%)	
IV	8 (12.7%)	1 (1.5%)	

Notes: Chi-square test or Fisher exact probability test, as appropriate, were used to compare the difference in categorical variables among different groups. Student *t* test or Mann–Whitney *U*-test, as appropriate, were used to compare the difference in continuous variables.
Abbreviations: MVI, microvascular invasion; WBC, white blood cell count; RBC, red blood cell count; HB hemoglobin; PLT, platelets; PT, prothrombin time;INR, international normalized ratio of prothrombin; APTT, activated partial thromboplastin time, FIB, fibrinogen, ALT, alanine aminotransferase; AST, aspartate aminotransaminase; ALB, albumin; GLB, globulin; ALP, alkaline phosphatase; GGT, gamma-glutamyl transferase; TBIL, total bilirubin; Cr, creatinine; AFP, alpha-fetoprotein; CTP, Child-Turcotte-Pugh stage; MELD, model for end-stage liver disease score.

Interobserver Agreement Regarding MRI Features

The two radiologists showed moderate to excellent inter-observer agreement for the MRI features of HCC, with κ values in the range of 0.431–0.885 (Table 2). The best interobserver agreement was observed for satellite nodule (κ=0.885; 95% CI: 0.796–0.974). Moderate consistency was observed for peritumoral HBP hypointensity (κ=0.511; 95% CI: 0.339–0.682).

MRI Features of HCC That Identify MVI Status

In univariate analysis, corona enhancement (*P*=0.021) and peritumoral HBP hypointensity (*P*=0.021) were more common in the MVI-positive group than in the MVI-negative group (Table 3). In the multivariate analysis, corona enhancement

Table 2 The Interobserver Agreement of MRI Features

Characteristics	Weighted Kappa	95% CI
Tumor margin	0.747	0.626–0.867
Capsule	0.609	0.461–0.758
Mosaic sign	0.667	0.536–0.797
Intratumoral necrosis	0.794	0.687–0.900
Intratumoral bleeding	0.757	0.644–0.871
Intratumoral fat	0.530	0.324–0.737
Low vascular composition	0.591	0.469–0.713
Intratumoral artery	0.638	0.516–0.760
Satellite nodule	0.885	0.796–0.974
Corona enhancement	0.621	0.444–0.798
Peritumoral hypointensity on HBP	0.511	0.339–0.682
Increased uptake in HBP	0.431	0.153–0.709

Abbreviations: CI, confidence interval; HBP, hepatobiliary phase.

Table 3 MRI Features of MVI-Positive and MVI-Negative HCCs

Characteristics	Total Patients (n=130)	MVI Positive (n=63)	MVI Negative (n=67)	P value
Tumor diameter (cm)	3.80(2.30–6.30)	4.30(2.65–6.10)	3.30(1.85–5.20)	0.116
Tumor margin				0.802
Smooth	44(33.8%)	22(34.9%)	22(32.8%)	
Nonsmooth	86(66.2%)	41(65.1%)	45(67.2%)	
Capsule				0.182
Absent	27(20.8%)	10(15.9%)	17(25.4%)	
Present	103(79.2%)	53(84.1%)	50(74.6%)	
Mosaic sign				0.230
Absent	71(54.6%)	31(49.2%)	40(59.7%)	
Present	59(45.4%)	32(50.8%)	27(40.3%)	
Intratumoral necrosis				0.781
Absent	80(61.5%)	38(60.3%)	42(62.7%)	
Present	50(38.5%)	25(39.7%)	25(37.3%)	
Intratumoral bleeding				0.781
Absent	80(61.5%)	38(60.3%)	42(62.7%)	
Present	50(38.5%)	25(39.7%)	25(37.3%)	
Intratumoral fat				0.946
Absent	107(82.3%)	52(82.5%)	55(82.7%)	
Present	23(17.7%)	11(17.5%)	12(17.9%)	
Low vascular composition				0.649
<20%	43(33.1%)	21(33.3%)	22(32.8%)	
20–50%	50(38.5%)	22(34.9%)	28(41.8%)	
>50%	37(28.5%)	20(31.7%)	17(25.4%)	
Intratumoral artery				0.057
Absent	73(56.2%)	30(47.6%)	43(64.2%)	
Present	57(43.8%)	33(52.4%)	24(35.8%)	
Satellite nodule				0.822
Absent	92(70.8%)	44(69.8%)	48(71.6%)	
Present	38(29.2%)	19(30.2%)	19(28.4%)	
Corona enhancement				0.021
Absent	109(83.8%)	48(76.2%)	61(91.0%)	
Present	21(16.2%)	15(23.8%)	6(9.0%)	

(*Continued*)

Table 3 (Continued).

Characteristics	Total Patients (n=130)	MVI Positive (n=63)	MVI Negative (n=67)	*P* value
Peritumoral hypointensity on HBP				0.021
Absent	109(83.8%)	48(76.2%)	61(91.0%)	
Present	21(16.2%)	15(23.8%)	6(9.0%)	
Increased uptake in HBP				0.719
Absent	122(93.8%)	60(95.2%)	62(92.5%)	
Present	8(6.2%)	3(4.8%)	5(7.5%)	

Notes: Chi-square test or Fisher exact probability test, as appropriate, were used to compare the difference in categorical variables among different groups. Mann–Whitney *U*-test was used to compare the difference in continuous variables.
Abbreviations: MVI, microvascular invasion; HBP, hepatobiliary phase.

(OR,3.019; 95% CI: 1.071–8.512; *P*=0.037) and peritumoral HBP hypointensity (OR, 3.019; 95% CI: 1.071–8.512; *P*=0.037) were independent predictors of MVI-positive status. The sensitivity, specificity, PPV, NPV, and AUROC of these two features for identifying MVI were 23.80%, 91.04%, 71.23%, 55.96%, and 0.574, respectively (representative images: Figure 2a and b).

Characteristics of Patients Without Peritumoral HBP Hypointensity

The median age of the 109 patients without peritumoral HBP hypointensity was 56.0 years (IQR 49.0–64.0) and 94 (86.2%) were male. As in the entire study cohort, there were no significant differences in any of the clinical or pathological characteristics between the MVI-positive and MVI-negative groups in patients without peritumoral HBP hypointensity, except for Edmondson grades III and IV (Table S3).

In patients without peritumoral HBP hypointensity, the only significant difference in MRI features between the MVI-positive and MVI-negative groups was the presence of radiological capsule (Table 4). The sensitivity, specificity, PPV,

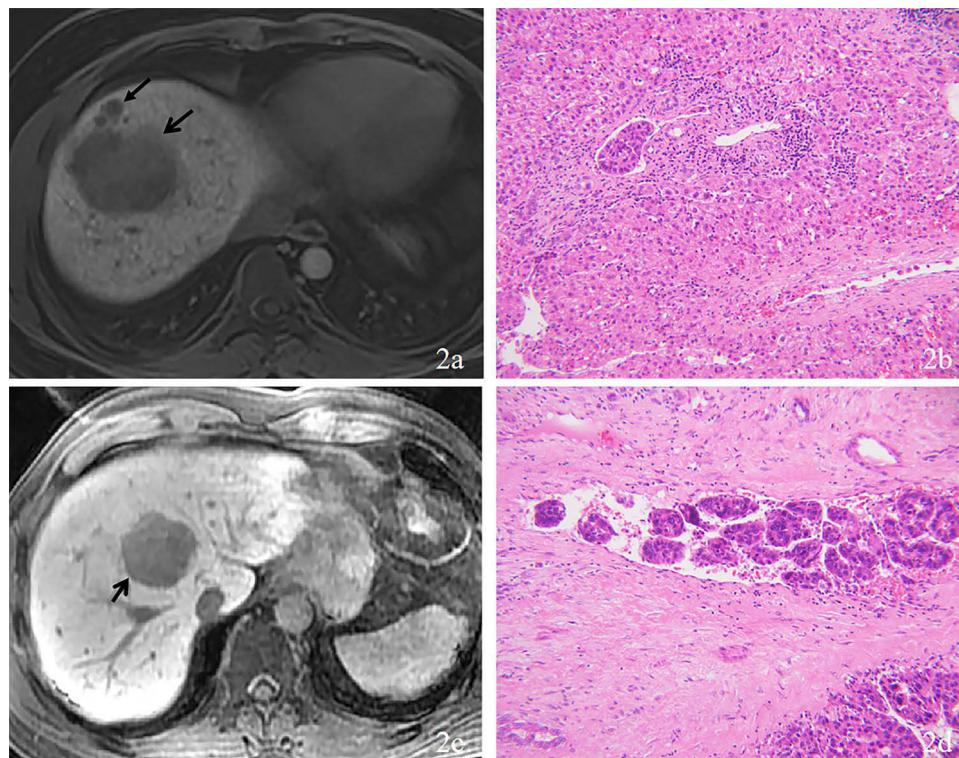**Figure 2** Representative MRI features associated with histopathological findings. HBP images (**a**) for a 29-year-old male patient showing peritumoral HBP hypointensity (arrow) and satellite nodule (arrowhead). Hepatocellular carcinoma with MVI-positive was confirmed by histopathology (**b**). HBP images (**c**) for a 41-year-old male patient showing a radiological capsule (arrow) without peritumoral HBP hypointensity. Hepatocellular carcinoma with MVI-positive was confirmed by histopathology (**d**).
Abbreviations: HBP, hepatobiliary phase; MVI, microvascular invasion.

Table 4 MRI Features of MVI-Negative and MVI-Positive HCCs in Subgroup Without Peritumoral HBP Hypointensity

Characteristics	Total Patients (n=109)	MVI Positive (n=48)	MVI Negative (n=61)	P value
Tumor diameter (cm)	3.40(2.20–5.60)	3.45(2.25–5.55)	3.40(2.10–5.60)	0.116
Tumor margin				0.579
Smooth	40(36.7%)	19(39.6%)	21(34.4%)	
Nonsmooth	69(63.3%)	29(60.4%)	40(65.6%)	
Capsule				0.038
Absent	21(19.5%)	5(10.4%)	16(26.2%)	
Present	88(80.7%)	43(89.6%)	45(73.8%)	
Mosaic sign				0.284
Absent	63(57.8%)	25(52.1%)	38(62.3%)	
Present	46(42.2%)	23(47.9%)	23(37.7%)	
Intratumoral necrosis				0.255
Absent	70(64.2%)	28(58.3%)	42(68.9%)	
Present	39(35.8%)	20(41.7%)	19(31.1%)	
Intratumoral bleeding				0.773
Absent	72(66.1%)	31(64.6%)	41(67.2%)	
Present	37(33.9%)	17(35.4%)	20(32.8%)	
Intratumoral fat				0.406
Absent	107(82.6%)	38(79.2%)	52(85.2%)	
Present	23(17.4%)	10(20.8%)	9(14.8%)	
Low vascular composition				0.782
<20%	40(36.7%)	18(37.5%)	22(36.1%)	
20–50%	40(36.7%)	16(33.3%)	24(39.3%)	
>50%	19(26.6%)	14(29.2%)	15(24.6%)	
Intratumoral artery				0.241
Absent	68(62.4%)	27(56.3%)	41(62.4%)	
Present	41(37.6%)	21(43.8%)	20(37.6%)	
Satellite nodule				0.884
Absent	81(74.3%)	36(75.0%)	45(73.8%)	
Present	28(25.7%)	12(25.0%)	16(26.2%)	
Corona enhancement				0.107
Absent	93(85.3%)	38(79.2%)	55(90.2%)	
Present	16(14.7%)	10(20.8%)	6(9.8%)	
Increased uptake in HBP				0.394
Absent	102(93.6%)	46(95.8%)	56(91.8%)	
Present	7(6.4%)	2(4.2%)	5(8.2%)	

Notes: Chi-square test or Fisher exact probability test, as appropriate, were used to compare the difference in categorical variables among different groups. Mann–Whitney *U*-test was used to compare the difference in continuous variables.
Abbreviations: MVI, microvascular invasion; HBP, hepatobiliary phase.

NPV, and AUROC of the radiological capsule for identifying MVI-positive HCC in this subgroup were 89.58%, 26.23%, 48.86%, 76.19%, and 0.579, respectively (representative images: Figure 2c and d).

MRI Features for Predicting Intrahepatic Recurrence

During a median follow-up period of 11 months (range, 1–56 months; IQR, 4–20 months), intrahepatic recurrence was diagnosed in 51 patients (39.3%). The median time to intrahepatic recurrence after curative hepatic resection was 7 months (range, 1–47 months; IQR, 3–13 months). Kaplan–Meier curves showed that intrahepatic RFS was shorter in patients with peritumoral HBP hypointensity than in those without (Figure 3, $P<0.001$). After adjusting potential confounders of age, gender, tumor size, and other radiological features, peritumoral HBP hypointensity (HR: 2.381, 95% CI: 1.162–4.881, $P=0.018$) remained significantly associated with shorter intrahepatic RFS (Table S4).
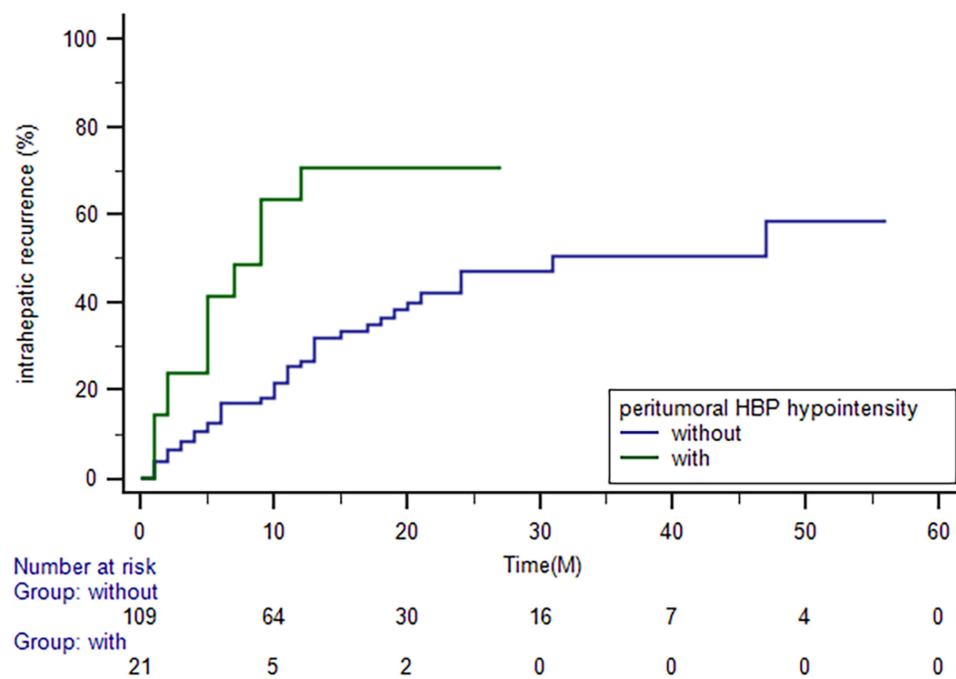
Figure 3 Kaplan–Meier curves showing recurrence-free survival in patients with and without peritumoral hepatobiliary phase hypointensity.

In patients without peritumoral HBP hypointensity, subgroup analysis showed that tumor size >5 cm (*P*=0.001), non-smooth margins (*P*=0.040), mosaic sign (*P*=0.040), necrosis (*P*=0.009), and satellite nodule (*P*<0.001) were prognostic factors for intrahepatic RFS. However, only satellite nodule (HR: 3.324, 95% CI: 1.733–6.378, *P*<0.001) was identified as an independent prognostic factor for intrahepatic RFS in multivariate Cox regression analysis (Table 5).

As shown in Figure 4, intrahepatic RFS was similar in patients without peritumoral HBP hypointensity who had satellite nodule to that in patients with peritumoral HBP hypointensity (*P*=0.693). However, intrahepatic RFS was significantly shorter in both cohorts than that in patients without either of these MRI features (*P*<0.001) (representative images: Figure 5).

Two Stepwise Flowchart for Prediction of Intrahepatic Recurrence

To facilitate clinical use and improve performance, a two-step flowchart incorporating peritumoral HBP hypointensity and satellite nodule was developed to stratify intrahepatic recurrence risk (Figure 6). Patients without peritumoral HBP hypointensity and satellite nodule had a low risk of intrahepatic recurrence, whereas those at a high risk (47/130, 36.2%) had an increased risk of intrahepatic recurrence. Using the two-step flowchart, 26 (20%) of 130 patients were reassigned

Table 5 Univariate and Multivariate Cox Regression of MRI Features in Predicting Intrahepatic Recurrence in Subgroup Without Peritumoral HBP Hypointensity

Imaging Feature	Univariable Analysis		Multivariable Analysis	
	Hazard Ratio (95% CI)	*P* value	Hazard Ratio (95% CI)	*P* value
Tumors size > 5 cm	2.928(1.545–5.550)	0.001	–	–
Unsmooth margin	2.186(1.037–4.611)	0.040	–	–
Mosaic sign	1.964(1.032–3.737)	0.040	–	–
Necrosis	2.341(1.242–4.411)	0.009	–	–
Satellite nodule	3.324(1.733–6.378)	<0.001	3.324(1.733–6.378)	<0.001

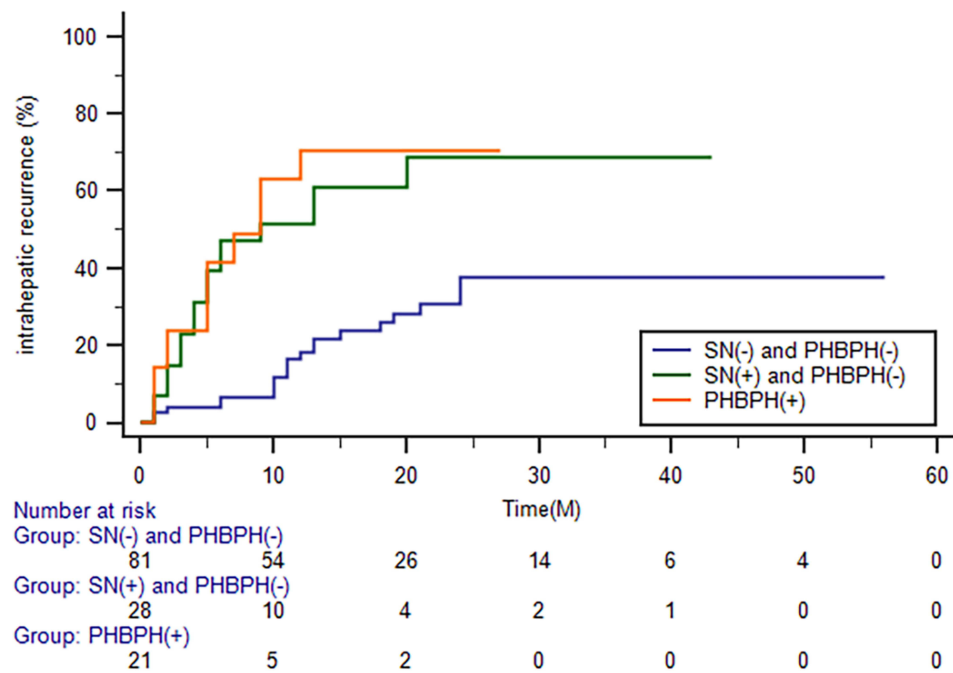**Abbreviations**: HBP, hepatobiliary phase; CI, confidence interval.

Figure 4 Kaplan–Meier curves showing recurrence-free survival in patients without peritumoral HBP hypointensity (PHBPH) and satellite nodule (SN), with SN but without PHBPH and with PHBPH.
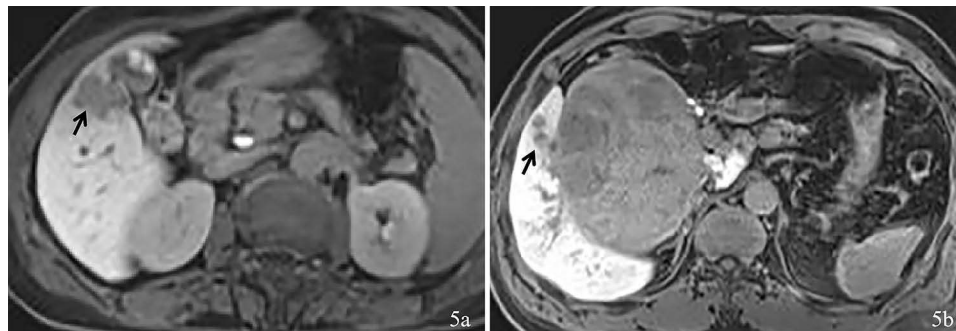

Figure 5 Representative MRI features associated with recurrence-free survival. HBP images (**a**) for a 60-year-old female patient showing an irregularly hypointense tumor (arrow) but without peritumoral HBP hypointensity or a satellite nodule. Tumor recurrence has not been found after 28 months of follow-up. HBP images (**b**) for a 50-year-old male patient showing multiple satellite nodules (arrow) around the tumor without peritumoral HBP hypointensity. Tumor recurrence was detected 4 months after curative resection.

as high-risk for intrahepatic recurrence, which was a significant improvement when compared with peritumoral HBP hypointensity alone ($P<0.001$).

Discussion

The findings of this study confirm that peritumoral HBP hypointensity is an important MRI feature that can be used to preoperatively predict pathological MVI and shorter intrahepatic RFS and that the presence of a radiological capsule can help to predict MVI status in patients without peritumoral HBP hypointensity. However, only the presence of satellite nodule was identified as an independent risk factor for intrahepatic RFS in this subgroup after univariate and multivariate Cox regression analyses.

Previous studies have established that the presence of MVI is one of the key factors in early recurrence of HCC and poor outcomes after curative liver resection or liver transplantation.[13] Preoperative assessment of MVI is important for accurate selection of candidates for the various treatment options. For example, studies in which MVI status was
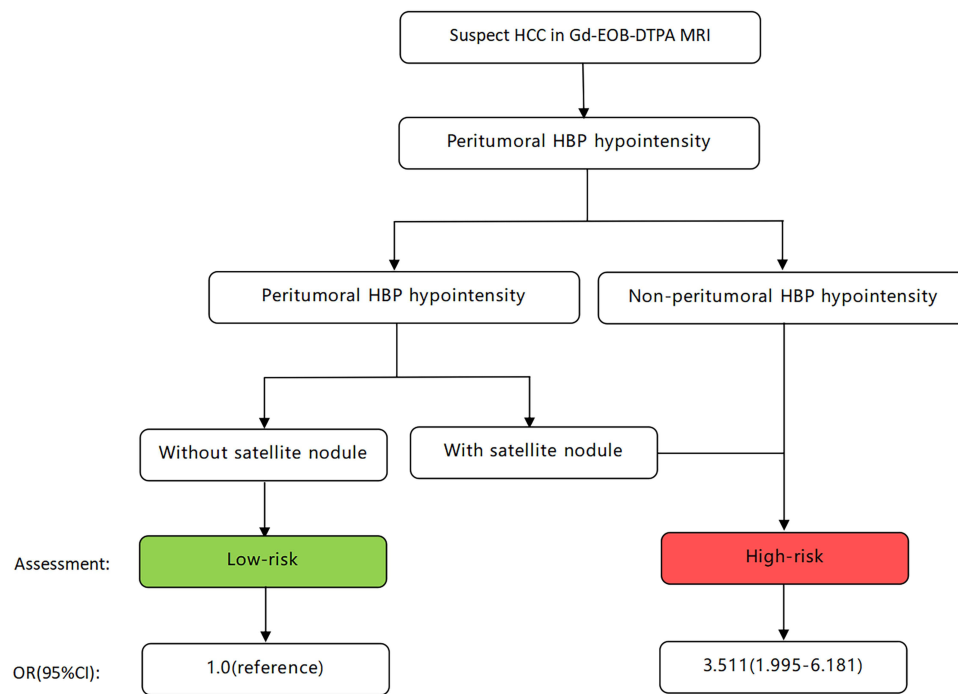
Figure 6 Two stepwise flowchart incorporating peritumoral hepatobiliary phase hypointensity and satellite nodule for stratification of the risk of intrahepatic recurrence. Recurrence-free survival was significantly shorter in patients with high-risk hepatocellular carcinoma than in those with low-risk hepatocellular carcinoma (hazard ratio 3.511, 95% confidence interval 1.995–6.181, *P*<0.001).

evaluated preoperatively found that the rate of early recurrence was lower after surgical resection than after radio-frequency ablation and that anatomical resection was superior to nonanatomical resection.[14–17] Therefore, the development of noninvasive methods for preoperative prediction of MVI status has become an important research topic in recent years. The features of HCC observed on Gd-EOB-DTPA-enhanced MRI were confirmed to be associated with MVI status. Our finding that corona enhancement and peritumoral HBP hypointensity are independent predictors of MVI is consistent with reports by Lee et al and Zhang et al[15,18] For MVI-positive HCCs, local tumor invasion or infiltration of tumor cells into vessels could impair the function of peritumoral hepatocytes, which would result in impaired OATP transporter expression and decreased uptake of Gd-EOB-DTPA in the peritumoral region, that is, peritumoral HBP hypointensity.[19] However, when infiltration of tumor cells in vessels is limited, impairment of OATP transporter function is also limited, as is the likelihood of peritumoral HBP hypointensity. Furthermore, HCCs with coactivation of Wnt/β-catenin signaling and hepatocyte nuclear factor 4α could induce higher OATP expression and manifest as peritumoral HBP hyperenhancement.[20] Therefore, peritumoral HBP hypointensity would be a good indicator for ruling in MVI rather than ruling it out. Our finding that the sensitivity of peritumoral HBP hypointensity in identifying MVI was quite low (23.80%) supports this theory. Almost three-quarters of the MVI-positive HCCs were missed when using this feature alone. Therefore, there is a need to explore other MRI features to identify MVI-positive HCC in patients without peritumoral HBP hypointensity.

The presence of a radiological capsule is a MRI characteristic that has been controversial in terms of predicting MVI status. Some studies have found that it is a valuable predictor of MVI-positive HCC, while others have not.[21–24] Interestingly, in our study, a radiological capsule could predict MVI in patients without peritumoral HBP hypointensity, but not in the overall study cohort. A possible explanation for this finding is that peritumoral HBP hypointensity was significantly more common in patients with MVI-positive HCC than in MVI-negative HCC in those patients without a radiological capsule (50.0% vs 5.8%, *P*=0.015). After removal of patients with peritumoral HBP hypointensity, there was a marked decrease in the proportion of patients with MVI-positive HCC without a radiological capsule. Therefore, the absence of a tumor capsule in this subgroup strongly indicates MVI-negative status and could be used as a rule-out

indicator. This is consistent with our finding that the presence of a radiological capsule has a relatively high NPV for predicting MVI-positive HCC in patients without peritumoral HBP hypointensity.

Peritumoral HBP hypointensity in HCC is not only associated with an increased risk of MVI but is also an established adverse prognostic imaging feature for early tumor recurrence after curative hepatic resection and liver transplantation.[19,25] In our study, intrahepatic RFS was significantly shorter in patients with peritumoral HBP hypointensity than in patients without this feature. However, given the relatively low frequency of peritumoral HBP hypointensity, it is necessary to explore other supplementary MRI features that could predict postoperative recurrence. Our study demonstrated that satellite nodule was an independent risk factor for intrahepatic RFS in patients without peritumoral HBP hypointensity. To the best of our knowledge, this is the first study to explore the risk of tumor recurrence in patients without peritumoral HBP hypointensity. The effect of satellite nodule on tumor recurrence has been demonstrated in previous studies. Mulé et al found that satellite nodule was independently associated with both early and overall tumor recurrence.[26] Similarly, Kim et al identified the presence of satellite nodule and peritumoral HBP hypointensity as independent factors associated with tumor recurrence after liver transplantation.[27] These studies strongly support our findings. Moreover, intrahepatic RFS was comparable between patients with peritumoral HBP hypointensity and those with satellite nodule but without peritumoral HBP hypointensity. Therefore, we established a two-step flowchart based on MRI features for the prediction of early hepatic recurrence, which showed good performance in risk assessment.

Interobserver variability is a major concern in terms of the reliability of the features seen on preoperative MRI images when used as a decision-making tool. In our study, the two radiologists yielded moderate to excellent agreement (κ=0.431–0.885) for MRI features of HCC, which is similar to the results reported by Lee et al (κ 0.64–0.88).[28] However, Min et al and Kim et al reported relatively lower κ values (0.38–0.47 and 0.53–0.59, respectively).[27,29] The good interobserver agreement in our study might be attributed to the discussion and case training on MRI features prior to formal assessment.

This study has several limitations. First, it had a single-center retrospective design and small sample size; therefore, there is a possibility of selection bias. Therefore, the results require confirmation in a larger multicenter prospective study. Second, the follow-up duration was relatively short and a proportion of patients were lost to follow-up, which may have diminished the strength of our results. However, most early intrahepatic HCCs occurred in the first year, similar to our data. Third, the main etiology of liver disease in our study was chronic hepatitis, particularly chronic hepatitis B. Further investigations in populations with different underlying causes are required.

Conclusion

In conclusion, we found peritumoral HBP hypointensity to be an important MRI feature for identifying MVI status and early intrahepatic recurrence but with low sensitivity. In patients without peritumoral HBP hypointensity, the presence of a radiological capsule may be useful for identifying the MVI status, whereas satellite nodule may be an independent risk factor for shorter intrahepatic RFS. The use of our two stepwise flowchart that incorporates peritumoral HBP hypointensity and satellite nodule could significantly improve the detection rate of high-risk HCC, which could assist clinicians in treatment decision-making.

Abbreviations

HCC, hepatocellular carcinoma; MVI, microvascular invasion; Gd-EOB-DTPA, gadolinium ethoxybenzyl diethylenetriamine pentaacetic acid; OATP, organic anion-transporting polypeptide; HBP, hepatobiliary phase; WBC, white blood cell count; RBC, red blood cell count; HB, hemoglobin; PLT, platelets; PT, prothrombin time; INR, international normalized ratio of prothrombin; APTT, activated partial thromboplastin time; FIB, fibrinogen; AST, aspartate aminotransferase; ALT, alanine transaminase; ALB, albumin; GLB, globulin; ALP, alkaline phosphatase; GGT, gamma-glutamyl transferase; TBIL, total bilirubin; Cr, creatinine; AFP, alpha-fetoprotein; CTP, Child-Turcotte-Pugh stage; MELD, model for end-stage liver disease score; AASLD, American association for the study of liver disease; RFS, recurrence-free survival; ROC, receiver operating characteristic; AUROC, area under ROC curve; OR, odds ratio; CI, confidence interval; PPV, positive predictive value; NPV, negative predictive value; HR, hazard ratio.

Data Sharing Statement

The datasets used and/or analyzed in this study are available from the corresponding authors on reasonable request.

Ethics Approval and Informed Consent

The studies involving human participants were reviewed and approved by the ethics committee of the Second Affiliated Hospital of Guangzhou University of Chinese Medicine (BE2022-226). The study was completed in accordance with the Declaration of Helsinki, and all patient data are treated confidentially. The requirement for written informed consent was waived by the Institutional Review Board in view of the retrospective observational nature of the research. Before Gd-EOB-DTPA enhanced MRI and curative hepatic resection, subjects received full information about indications, risks, and alternatives and then signed the written informed consent.

Acknowledgments

Author Contributions

Conceptualization, Zhiyuan Chen, Xiaohuan Li, and Yupin Liu; design, Zhiyuan Chen, Dongjing Zhou, and Yupin Liu; Resources, Zhiyuan Chen, Yan Zhang, and Yupin Liu; execution, Xiaohuan Li, Yu Zhang, Yiming Yang, Yu Yang, and Shuping Zhang; acquisition of data, Xiaohuan Li, Yu Zhang, Yiming Yang, Yan Zhang, and Yu Yang; Formal Analysis, Zhiyuan Chen, Xiaohuan Li, Yan Zhang, and Dongjing Zhou;; Writing – Original Draft, Zhiyuan Chen, Xiaohuan Li, Yu Zhang, Yiming Yang, Yan Zhang, Yu Yang, and Shuping Zhang; Writing – Review & Editing, Zhiyuan Chen, Dongjing Zhou, and Yupin Liu. All authors made substantial contributions to conception and design, acquisition of data, or analysis and interpretation of data; took part in drafting the article or revising it critically for important intellectual content; agreed to submit to the current journal; gave final approval of the version to be published; and agree to be accountable for all aspects of the work.

Funding

Disclosure

The authors report no conflicts of interest in this work.

References

1. Vogel A, Meyer T, Sapisochin G, Salem R, Saborowski A. Hepatocellular carcinoma. *Lancet*. 2022;400(10360):1345–1362. doi:10.1016/S0140-6736(22)01200-4
2. Calderaro J, Seraphin TP, Luedde T, Simon TG. Artificial intelligence for the prevention and clinical management of hepatocellular carcinoma. *J Hepatol*. 2022;76(6):1348–1361.
3. Rumgay H, Arnold M, Ferlay J, et al. Global burden of primary liver cancer in 2020 and predictions to 2040. *J Hepatol*. 2022;77(6):1598–1606. doi:10.1016/j.jhep.2022.08.021
4. Erstad DJ, Tanabe KK. Prognostic and therapeutic implications of microvascular invasion in hepatocellular carcinoma. *Ann Surg Oncol*. 2019;26(5):1474–1493. doi:10.1245/s10434-019-07227-9
5. Beaufrère A, Caruso S, Calderaro J, et al. Gene expression signature as a surrogate marker of microvascular invasion on routine hepatocellular carcinoma biopsies. *J Hepatol*. 2022;76(2):343–352. doi:10.1016/j.jhep.2021.09.034
6. Wu Y, Zhu M, Liu Y, Cao X, Zhang G, Yin L. Peritumoral imaging manifestations on Gd-EOB-DTPA-enhanced MRI for preoperative prediction of microvascular invasion in hepatocellular carcinoma: a systematic review and meta-analysis. *Front Oncol*. 2022;12:907076. doi:10.3389/fonc.2022.907076
7. Hong SB, Choi SH, Kim SY, et al. MRI features for predicting microvascular invasion of hepatocellular carcinoma: a systematic review and meta-analysis. *Liver Cancer*. 2021;10(2):94–106. doi:10.1159/000513704
8. Rhee H, Cho ES, Nahm JH, et al. Gadoxetic acid-enhanced MRI of macrotrabecular-massive hepatocellular carcinoma and its prognostic implications. *J Hepatol*. 2021;74(1):109–121. doi:10.1016/j.jhep.2020.08.013
9. Kang HJ, Kim H, Lee DH, et al. Gadoxetate-enhanced MRI features of proliferative hepatocellular carcinoma are prognostic after surgery. *Radiology*. 2021;300(3):572–582. doi:10.1148/radiol.2021204352
10. Elsayes KM, Kielar AZ, Chernyak V, et al. LI-RADS: a conceptual and historical review from its beginning to its recent integration into AASLD clinical practice guidance. *J Hepatocell Carcinoma*. 2019;6:49–69. doi:10.2147/JHC.S186239

11. Kim WR, Mannalithara A, Heimbach JK, et al. MELD 3.0: the model for end-stage liver disease updated for the modern era. *Gastroenterology.* 2021;161(6):1887–1895.e4. doi:10.1053/j.gastro.2021.08.050

12. Benchoufi M, Matzner-Lober E, Molinari N, Jannot AS, Soyer P. Interobserver agreement issues in radiology. *Diagn Interv Imaging.* 2020;101 (10):639–641. doi:10.1016/j.diii.2020.09.001

13. He T, Zou J, Sun K, et al. Global research status and frontiers on microvascular invasion of hepatocellular carcinoma: a bibliometric and visualized analysis. *Front Oncol.* 2022;12:1037145. doi:10.3389/fonc.2022.1037145

14. Bai S, Yang P, Xie Z, et al. Preoperative estimated risk of microvascular invasion is associated with prognostic differences following liver resection versus radiofrequency ablation for early hepatitis b virus-related hepatocellular carcinoma. *Ann Surg Oncol.* 2021;28(13):8174–8185. doi:10.1245/s10434-021-09901-3

15. Lee S, Kang TW, Song KD, et al. Effect of microvascular invasion risk on early recurrence of hepatocellular carcinoma after surgery and radiofrequency ablation. *Ann Surg.* 2021;273(3):564–571. doi:10.1097/SLA.0000000000003268

16. Meng XP, Tang TY, Ding ZM, et al. preoperative microvascular invasion prediction to assist in surgical plan for single hepatocellular carcinoma: better together with radiomics. *Ann Surg Oncol.* 2022;29(5):2960–2970. doi:10.1245/s10434-022-11346-1

17. Zhang X, Li J, Shen F, Lau WY. Significance of presence of microvascular invasion in specimens obtained after surgical treatment of hepatocellular carcinoma. *J Gastroenterol Hepatol.* 2018;33(2):347–354. doi:10.1111/jgh.13843

18. Zhang L, Yu X, Wei W, et al. Prediction of HCC microvascular invasion with gadobenate-enhanced MRI: correlation with pathology. *Eur Radiol.* 2020;30(10):5327–5336. doi:10.1007/s00330-020-06895-6

19. Jiang H, Wei H, Yang T, et al. VICT2 trait: prognostic alternative to peritumoral hepatobiliary phase hypointensity in HCC. *Radiology.* 2023;307 (2):e221835. doi:10.1148/radiol.221835

20. Kitao A, Matsui O, Zhang Y, et al. Dynamic CT and gadoxetic acid-enhanced MRI characteristics of P53-mutated hepatocellular carcinoma. *Radiology.* 2023;306(2):e220531. doi:10.1148/radiol.220531

21. Tang M, Zhou Q, Huang M, et al. Nomogram development and validation to predict hepatocellular carcinoma tumor behavior by preoperative gadoxetic acid-enhanced MRI. *Eur Radiol.* 2021;31(11):8615–8627. doi:10.1007/s00330-021-07941-7

22. Zhang L, Lin JB, Jia M, et al. Clinical and imaging features preoperative evaluation of histological grade and microvascular infiltration of hepatocellular carcinoma. *BMC Gastroenterol.* 2022;22(1):369. doi:10.1186/s12876-022-02449-w

23. Li YM, Zhu YM, Gao LM, et al. Radiomic analysis based on multi-phase magnetic resonance imaging to predict preoperatively microvascular invasion in hepatocellular carcinoma. *World J Gastroenterol.* 2022;28(24):2733–2747. doi:10.3748/wjg.v28.i24.2733

24. Huang M, Liao B, Xu P, et al. Prediction of microvascular invasion in hepatocellular carcinoma: preoperative Gd-EOB-DTPA-dynamic enhanced MRI and histopathological correlation. *Contrast Media Mol Imaging.* 2018;2018:9674565. doi:10.1155/2018/9674565

25. Lee S, Kim KW, Jeong WK, et al. Gadoxetic acid-enhanced MRI as a predictor of recurrence of HCC after liver transplantation. *Eur Radiol.* 2020;30(2):987–995. doi:10.1007/s00330-019-06424-0

26. Mulé S, Galletto Pregliasco A, Tenenhaus A, et al. Multiphase liver MRI for identifying the macrotrabecular-massive subtype of hepatocellular carcinoma. *Radiology.* 2020;295(3):562–571. doi:10.1148/radiol.2020192230

27. Kim AY, Sinn DH, Jeong WK, et al. Hepatobiliary MRI as novel selection criteria in liver transplantation for hepatocellular carcinoma. *J Hepatol.* 2018;68(6):1144–1152. doi:10.1016/j.jhep.2018.01.024

28. Lee S, Kim SH, Lee JE, Sinn DH, Park CK. Preoperative gadoxetic acid-enhanced MRI for predicting microvascular invasion in patients with single hepatocellular carcinoma. *J Hepatol.* 2017;67(3):526–534. doi:10.1016/j.jhep.2017.04.024

29. Min JH, Lee MW, Park HS, et al. Interobserver variability and diagnostic performance of gadoxetic acid-enhanced MRI for predicting microvascular invasion in hepatocellular carcinoma. *Radiology.* 2020;297(3):573–581. doi:10.1148/radiol.2020201940